

Electronic Supplementary Information for Reshaping Sub-millimetre Bubbles from Spheres to Tori

Authors: Xujun Zhang,^{ab} Shane Jacobeen,^c Qiang Zhang,^d Brian Khau,^e Peter Yunker,^c
H. Jerry Qi,^d Saad Bhamla,^{*e} and Paul S. Russo^{*abf}

Affiliations:

^aSchool of Materials Science and Engineering, Georgia Institute of Technology, Atlanta, GA 30332, USA.

^bGeorgia Tech Polymer Network, Georgia Institute of Technology, Atlanta, GA 30332, USA.

^cSchool of Physics, Georgia Institute of Technology, Atlanta, GA 30332, USA.

^dWoodruff School of Mechanical Engineering, Georgia Institute of Technology, Atlanta, GA 30332, USA.

^eSchool of Chemical and Biomolecular Engineering, Georgia Institute of Technology, Atlanta, GA 30332, USA.

^fSchool of Chemistry and Biochemistry, Georgia Institute of Technology, Atlanta, GA 30332, USA.

*To whom correspondence may be addressed. Email: saadb@chbe.gatech.edu or paul.russo@mse.gatech.edu

This PDF file includes:

Figures S1 to S6

Legends for Movies S1 to S4

Surface energy estimate for protein detachment from the air-water interface

Other Supplementary Materials for this manuscript include the following:

Movies S1 to S4

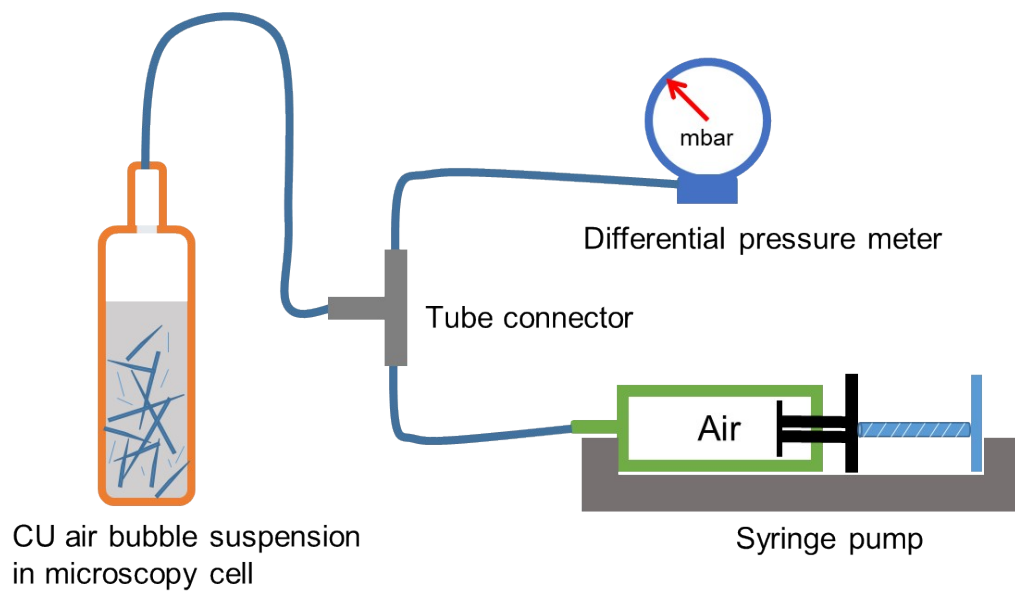


Fig. S1. Schematic of apparatus used to generate positive or negative pressure in the headspace of the microscopy cell containing *cerato-ulmin* dispersions.

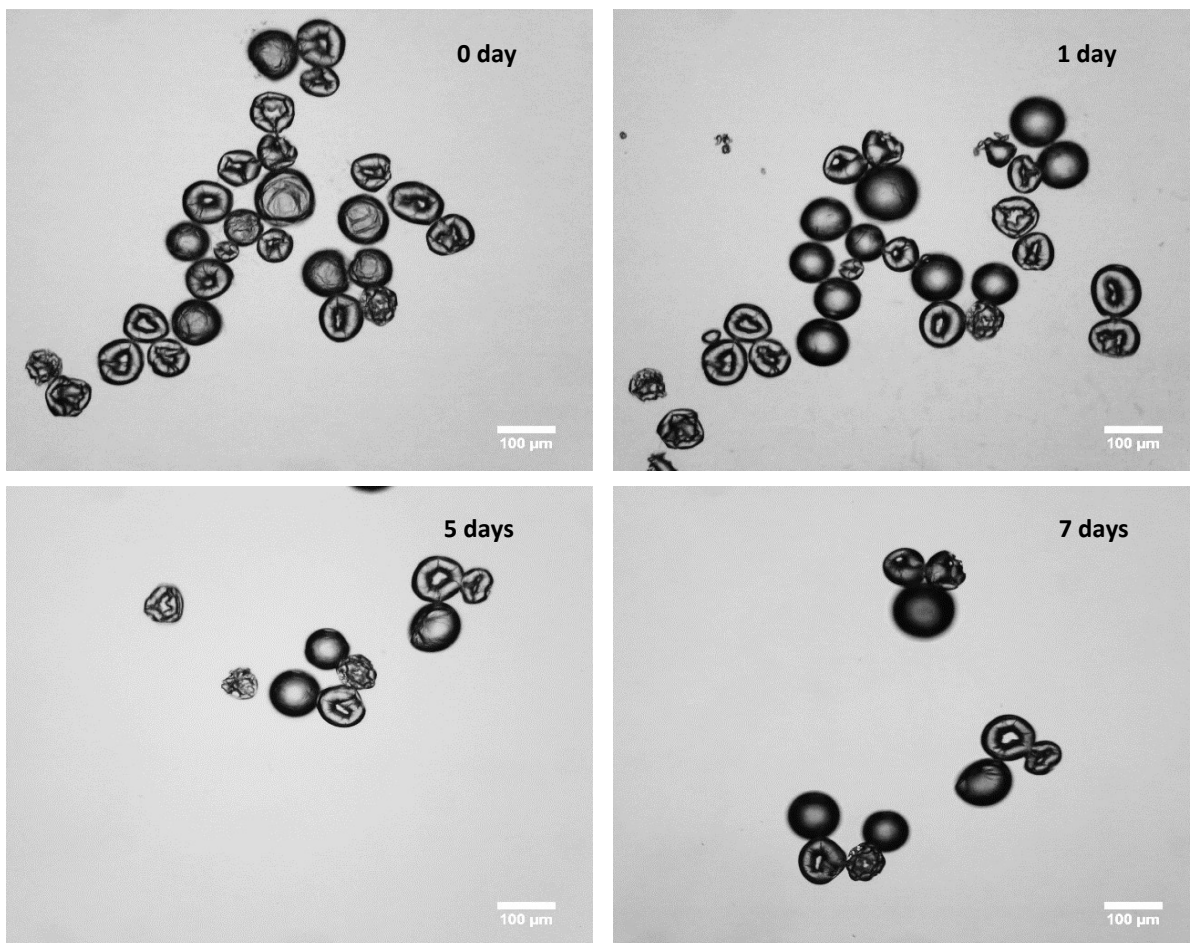


Fig. S2. The toroidal bubbles are stable for at least five days at ambient storage pressure.

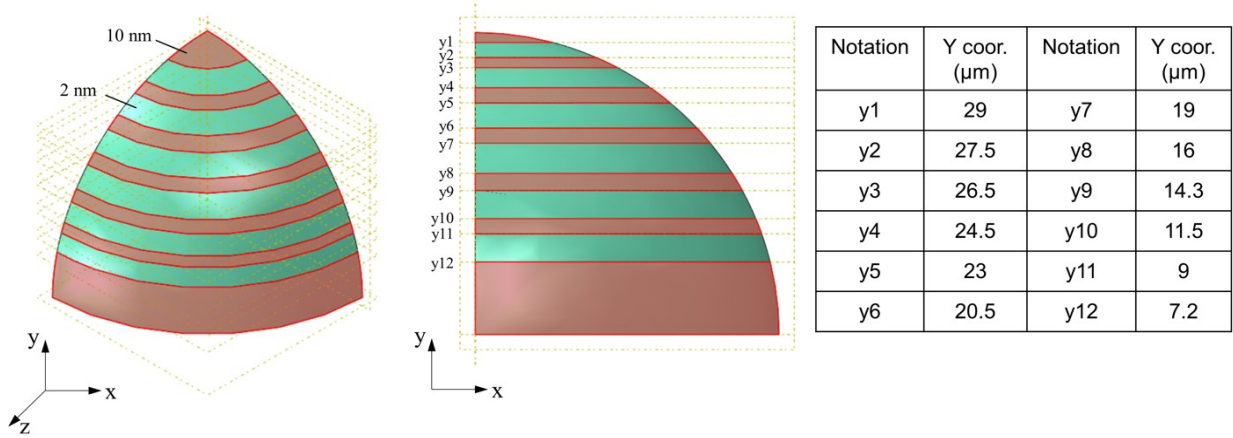


Fig. S3. Symmetric eighth geometric model and thickness region partition for finite element analysis.

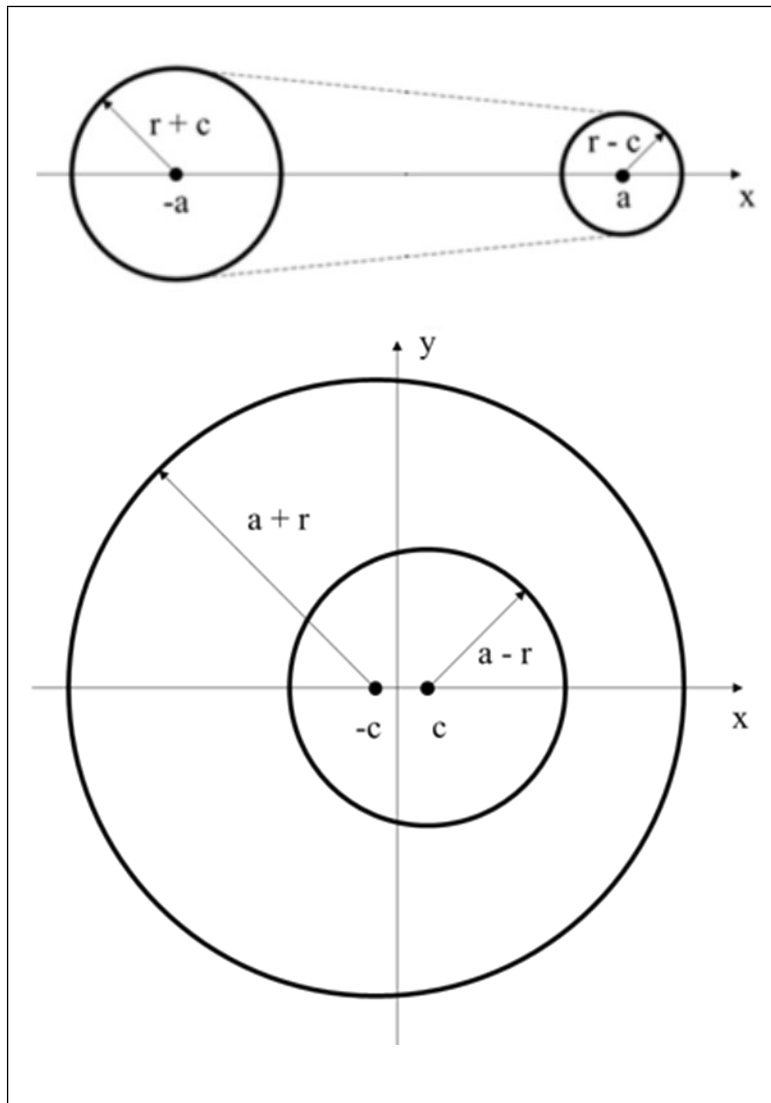


Fig. S4. Characterization of axially asymmetric genus 1 objects following reference (57). (A) Cross section of a Dupin cyclide in symmetry planes (vertical and horizontal slices through the middle).

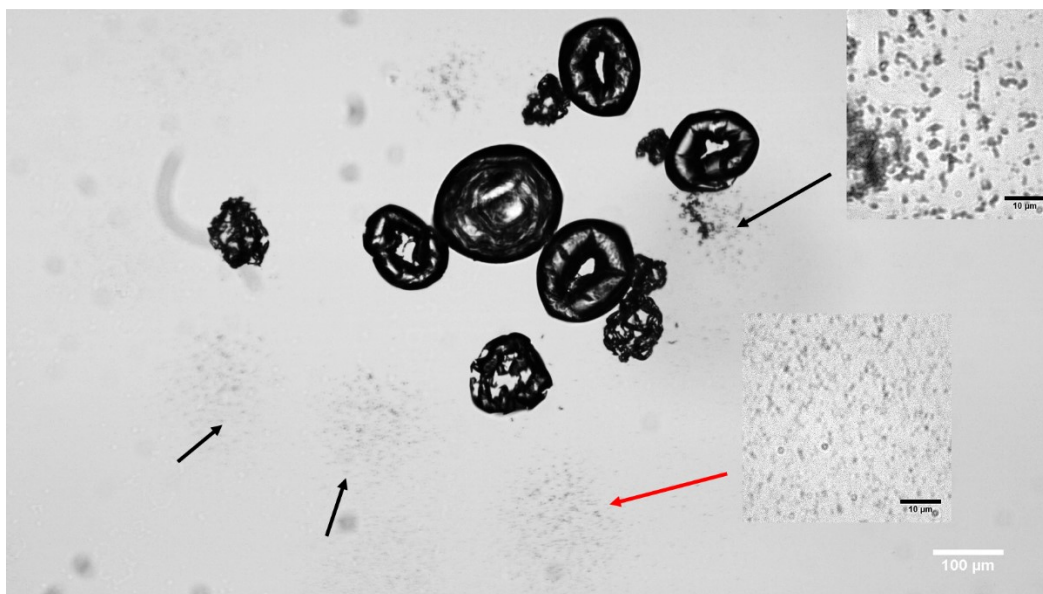


Fig. S5. CU-coated air bubbles fall apart into small debris (arrow indicated) as overpressure is supplied. Inset images show zoom-in view of two bubbles after falling apart.

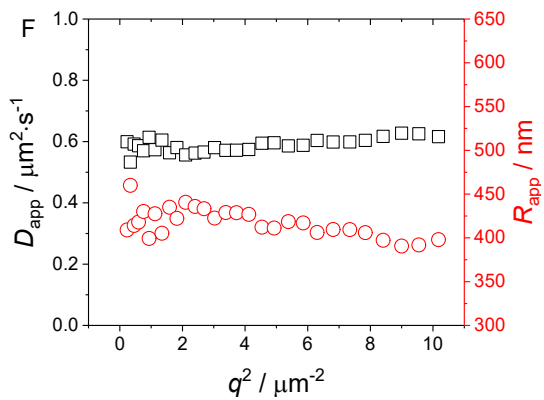
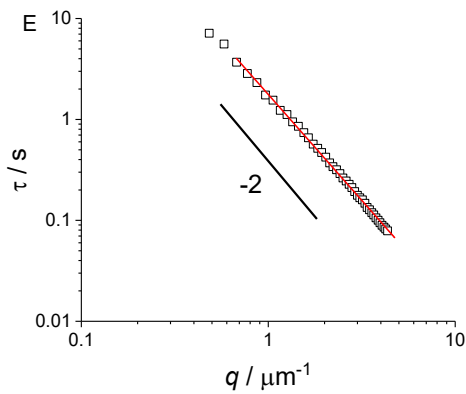
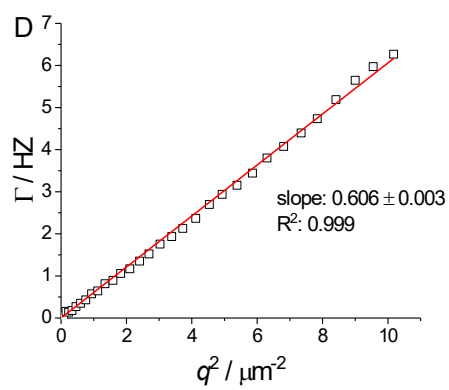
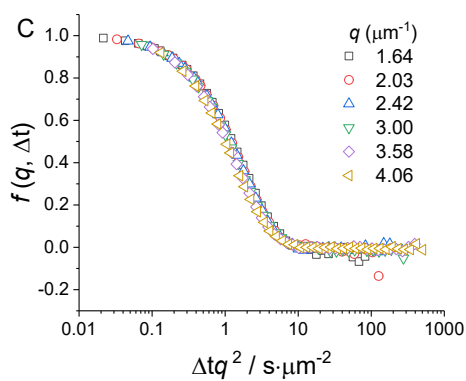
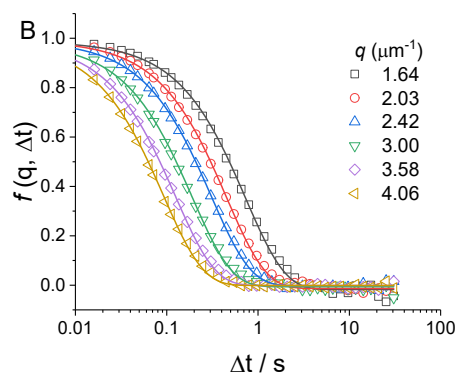
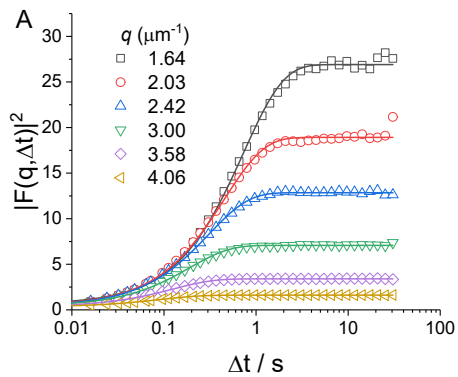


Fig. S6. DDM results from bubbles debris (red arrow) in Fig. S4. The DDM matrix $|F_D(q,\Delta t)|^2$ and normalized auto-correlation function $f(q,\Delta t)$ projected on Δt for different q indicate exponential growth or decay behavior, respectively. (A) Growth of $|F_D(q,\Delta t)|^2$ with delay time Δt for six values of q (μm^{-1}). The continuous lines are fits of the data. (B) Normalized auto-correlation function $f(q,\Delta t)$ extracted from $|F_D(q,\Delta t)|^2$ at various q versus Δt . Lines are exponential fits to the data. (C) $f(q,\Delta t)$ collapses when plotted as a function of $\Delta t q^2$. This scaling is compatible with a Brownian diffusive process. (D & E) Γ and τ are plotted against q^2 . (F) The bubble debris indicates characteristic Brownian diffusion, yielding a diffusion coefficient of $D_t = 0.61 \mu\text{m}^2/\text{s}$ and a corresponding uniform radius of 400 nm.

Energy of detachment from surface

We use the model of Prabhudesai et al. (Ref 44 of the main document) to estimate the free energy of CU molecule detachment from an air-water interface, assuming the CU single molecule is a solid, spherical particle with a diameter of D and contact angle of θ . The energy required to remove one CU molecule from the interface is expressed by ΔE_{da} ,

ΔE_{dw} and ΔE_d , where $\Delta E_{da} = \frac{1}{4}\pi D^2 \gamma_{aw} (1 - \cos \theta)^2$ is the free energy of particle detachment

into air, $\Delta E_{dw} = \frac{1}{4}\pi D^2 \gamma_{aw} (1 + \cos \theta)^2$ is the free energy of particle detachment into water and

$\Delta E_d = \frac{1}{4}\pi D^2 \gamma_{aw} (1 - |\cos \theta|)^2$ is the minimum energy for detachment into the bulk phase.

Using the value of $D = 2.64$ nm, the surface tension of clean air-water interface (γ_{aw}) of 72 mN/m, the free energy of CU detachment is calculated as a function of contact angle θ . The free energy required for CU detachment is at least 100 kT when $\theta = 90^\circ$, indicating the irreversible particulate adsorption at interfaces.

Movie S1.

Cerato-ulmin rodlike bubbles transition to spherical shapes upon pressure changes above the *cerato-ulmin* dispersion. Images were collected at 137 frames/second, then compiled into videos.

Movie S2.

Cerato-ulmin spherical bubbles transition to toroidal shapes following a prescribed pressure manipulation. Images were collected at 120 frames/second, then compiled into videos and played at a speed of 4 times faster than recorded.

Movie S3.

Cerato-ulmin spherical bubbles transition to toroidal shapes following a prescribed pressure manipulation. Images were collected at 120 frames/second, then compiled into videos and played at a speed of 8 times faster than recorded.

Movie S4.

Repeated shape transition from sphere to tori while applying pressure oscillation. Images were collected at 120 frames/second, then compiled into videos and played at a speed of 4 times faster than recorded.